

Characterization, microstructure, and gas sensitive response behavior of PEG/lithium salt polymer electrolyte films

Yanling Luo · Shuhong Wang · Zhanqing Li

Received: 3 May 2007 / Accepted: 22 August 2007 / Published online: 29 September 2007
© Springer Science+Business Media, LLC 2007

Abstract A composite polymer electrolyte film was prepared by dissolving polyethylene glycol (PEG) with different molecular weight in acetonitrile, and vapor-induced response behavior was investigated upon exposure to various chemical environments. The effect of lithium concentrations on ionic conductivity and response was discussed. The surface microporous structures and vapor sensitive conductivity of the films in the case of poly(vinylidene fluoride) (PVDF) were examined with the PVDF content changed. The crystalline and micro-phase isolation behavior were characterized by a differential scanning calorimeter, an environmental scanning electron microscope, a polarization microscope and a wide-angle X-ray diffraction. The experimental results indicated that PEG/Li⁺ salt composite films exhibited preferential responsive characteristics. The responsivities to ethanoic acid, chloroform, and acetone vapors were enhanced with molecular weight of PEG increased. The conductivity was increased at a higher lithium salt concentration, and also enhanced with PEG content increased, while the responsivities decreased. The formation of microporous structures on the surface of the mixed PEG/PVDF composite films enlarged their specific area and strikingly improved the responsive performances. The changes in conduction behavior were explained from the viewpoint of the swelling and free volume theories as well as a hydrogen bond interaction, combined with the structural and morphological analyses. The introduction of an ionogenic matter also has an important effect on ionic conductivity and responsiveness.

Introduction

The polymeric electrolyte, a polymer material with ionic conductivity, is an emerging electrolyte material developed in the 1970s. It has found wide applications in the aspects of electron, medical service, spatial technology, electro-induced color effect, photo-electricity chemistry and so on. Since Wright et al. discovered that the complex compound formed from polyethylene oxide (PEO) with an alkaline metal salt had ionic conductivity in 1973 [1], the polymer electrolyte composed of PEO-LiX salt system has received widespread attention for a long time. Moreover, it is possible to substitute liquid electrolytes in the traditional lithium ion battery, thus it becomes an electrolyte material in an entire solid state lithium ion polymer battery [2, 3]. In 1979, a Frenchman named Armand [4] proposed that a polyether-alkaline metal salt compound possessed ionic conductivity and film-formation properties and so on. This caused it to become a new kind of polymer solid electrolyte with potential application values. Nowadays a great research progress has already been made in the research and development of polymer solid electrolyte doped with various kinds of lithium salts, ranging from material synthesis to structural performances and the like [5, 6]. The technical patents related and technical progress in practical applications had also been reported.

Dong [7, 8] has started to examine the transportation mechanism of the matters in polymer electrolytes and the dynamics at solid–solid interfaces and so on since 1990s. The solid polymer electrolytes being investigated at the present time are mostly obtained by adding a little amount of salt into massive polymer matrices, namely a so-called “salt-in-polymer” system. This solid polymer electrolyte is mainly used in high energy density cells, electrochemistry installments and so on. The rapid development in modern

Y. Luo (✉) · S. Wang · Z. Li
School of Chemistry and Materials Science, Shaanxi Normal University, Xi'an 710062, P.R. China
e-mail: luoyl0401@yahoo.com.cn; luoyanl@snnu.edu.cn

science and technology has greatly impelled the advances in sensing materials and technologies [9–11]. Sensor technologies are essential in many fields such as life science, national defense, machine finishing, and chemistry survey. They are increasingly demanded to exhibit more functions and higher performances. Due to the limitations of materials producing the traditional chemistry sensors, however, further improvements have hardly been made in microminiaturization, automation, selectivity, stability, responsive time, sensitivity, service life. It can no longer meet the needs of the development of science and technology. Therefore, the development and applications of a new kind of sensing materials become increasingly significant.

Since Vaisala Corp in Finnish successfully developed Hunicap gas-sensitive sensor in 1978, the polymer sensitive sensors with outstanding performances have increasingly been thought much of in many fields. The so-called gas sensitive material is referred to as a kind of material, of which certain characteristic parameters like resistances, electric capacity, coefficient of dielectric loss, volume, and so on, changes with the environment atmosphere change. And it is an important constituent of sensitive sensors. The sensor element made from this kind of material may display an extraordinary physical function with which human or any other beings' sense of smell systems have. Therefore it is also called an electronic nose. It can be utilized to carry out specific chemistry or environment examination, ground mineral examination, solvent revelation detection, polymer chemical constitution analysis, and biomedicine domain, exhibiting a broad prospect. Since the performances of the materials directly affects the sensitivity, the response speed, the restoring performance and the responsivity as well as the life of the sensors, the development of sensing materials with ideal gas sensitive performances is always an important effort in material research area. The applications of the solid electric conduction polymer electrolytes to sensor fields have early been forecast, but the applied research concerned was not reported. Based on the above standpoint we selected a PEG/Li⁺ salt as an investigation system in the present work and prepared different solid polyelectrolyte films. A sensing material with optimal gas responsive characteristics was obtained by emphatically inspecting the effect of molecular weight of PEG, Li⁺ salt concentrations and morphology of the films on the conductivity and response kinetics.

Experimental details

Materials and reagents

Poly (ethylene glycol) (PEG) samples used in this study were commercial products with molecular weight of 1,000,

6,000, 12,000, and 20,000 as designated by the manufacturer, Shanghai Pudong Gaonan Chemical Factory and were dried in vacuum at 70 °C for 24 h before use. Poly(vinylidene fluoride) (PVDF, FR 902) was a granular product purchased from the Shanghai 3F New Materials Corp. Ltd., with molecular weight of $(4-6) \times 10^5$ and a density of $1.75 \sim 1.78 \text{ g cm}^{-3}$, used as received. LiClO₄, analytically pure, was supplied by the No. 2 Reagent Factory of Shanghai and were dried in vacuum at 120 °C for 24 h before use. Glycerol (a matter forming micropores) was supplied by the Xi'an Baqiao Chemical Reagent Factory. Acetonitrile, Carbonic allyl ester (PC), and dimethylformamide (DMF), all analytically pure, were obtained from the Xi'an Chemical Reagent Factory, used as received.

Experimental procedures

Preparation of LiClO₄/PEG electrolyte films

Different proportions of PEG and LiClO₄ salts treated above were dissolved in a calculated amount of acetonitrile so as to obtain a 28 wt% PEG solution. The solution was sufficiently stirred at room temperature for 3 h till it became clear. LiClO₄/PEG electrolyte film specimens with a thickness of around 0.1–0.2 mm were fabricated by dipping the above paste solution and drawing back quickly so as to deposit the paste onto a comb-like electrode, a copper electrode with dimensions of 6 mm × 6 mm with a ceramic substrate that was prepared by a screen-printing technique. In the meanwhile, the paste solution was cast on a flat glass plate. The solvent was naturally evaporated at room temperature for 24 h. Then the possible trace of residual solvent was evacuated from the film in vacuum at 40 °C for 48 h.

Preparation of PVDF/PEG/Li⁺ polymer electrolyte films

PVDF/PEG/Li⁺ films with and with no micropores were achieved by phase transition route given in the literature [12]. PEG and PVDF were dissolved in a mixed solvent consisting of DMF and glycerol in line with mass ratios of PVDF:PEG:glycerol:DMF = 1: x :(1 + x): $10 \times (1 + x)$ ($x = 0.5$ or 2). The solution was intensively stirred at 80 °C for 4 h till it became clear. The film specimens with the same thickness were fabricated according to the aforementioned method. Then the mixed solvent was removed in oven at 100 °C to prepare microporous films. Since DMF and glycerol are provided with different boiling points, DMF was first evaporated while glycerol was vaporized gradually. Therefore a large amount of micropores were

formed in the positions occupied by glycerol. After treated for 12 h, the specimens were removed from the oven and then dried in vacuum at 100 °C for 6 h in order to obtain stable film specimens. The film specimens were dipped and kept in a LiClO₄/PC electrolyte solution of 0.0057 mol L⁻¹ for 1 h. The electrolyte solution on the surface was sipped up by filter paper. Then a PVDF/PEG/Li⁺ electrolyte film specimen was obtained.

Measurements and characterization

Resistance measurements

The film element specimens were connected with a detector—a digital multimeter (Victor VC9808) manufactured by Shenzhen Victory Instrument Factory with a maximal range of $2.0 \times 10^9 \Omega$ to record the change in resistance of the specimens. The initial resistance (R_0) was measured in dry air at room temperature until the value was stabilized so as to exclude the effect of adventitious moisture absorption on response. Then the specimens were immediately transferred into the airtight conical flask full of pure solvent vapors at the bottom and the resistance change was recorded. The distance between the film element specimens and solvent surface is about 2 cm. The measurement of the electrical resistance-time response patterns of the film element specimens to various solvent vapors were carried out at room temperature. After stabilized for 5 min., the element specimens were taken out rapidly and the resistance variation was observed and recorded.

Wide angle X-ray diffraction (WAXD)

In order to inspect the crystalline information of the PEG polymeric film samples with different molecular weight and the PVDF/PEG film samples with varying proportions, WAXD studies were performed on a Rigaku Co. D/Max-2550 VB+/PC automatic X-ray diffraction equipment made in Japan employing Cu radiation at a voltage of 40 kV and current of 40 mA, with scanning range from 5 to 50 deg and scanning rate 4 deg min⁻¹.

Differential scanning calorimeter (DSC)

A Q1000DSC+LNCS+FACS Q600SDT thermal analyzer (the TA Co. of America) was used to measure the thermal properties of the samples. The differential scanning calorimetry (DSC) scans of all samples were carried out over a

range of temperature from -100 to 220 °C at a heating rate of 10 °C min⁻¹ in N₂ atmosphere (40 ml min⁻¹).

Polarization microscope (POM) analysis

A cold/heat polarization microscope (model LEICA-DMLP EC600) manufactured by the Leica Corp. of Germany was used to examine the crystalline configuration and microphase separation behavior of the film samples with different molecular weight and the PVDF/PEG film samples with varying proportions.

Environmental scanning electron microscope (ESEM)

The surface morphologies (pore distribution and structures) of the PVDF/PEG film samples with varying proportions were observed using a Quanta 200 ESEM produced by the Philips-FEI Corp, Holland, with an operating voltage of 20 kV.

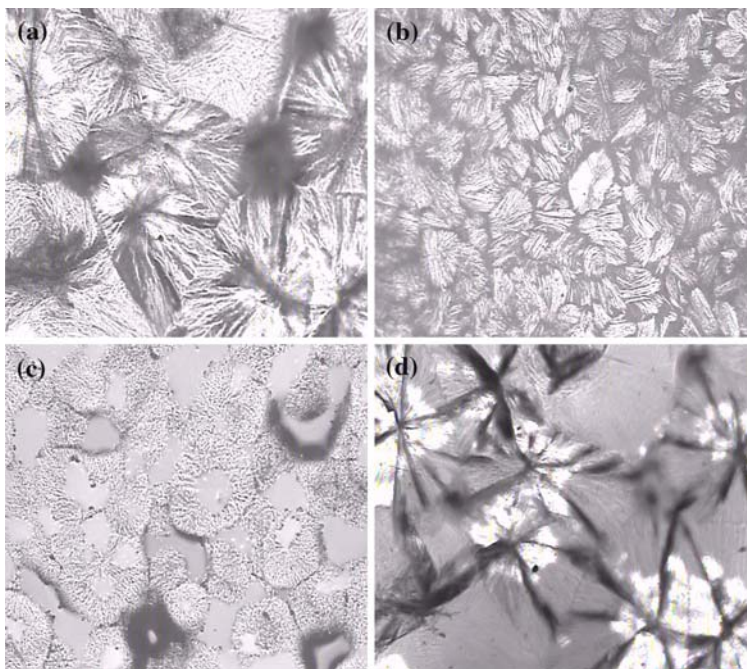
Results and discussion

POM analysis

Figure 1 shows a group of optical or POM photographs of PEG (with molecular weight of 12,000)/Li⁺ polymer films obtained from acetonitrile solution with varying Li⁺ salt concentrations annealed at 40 °C for 24 h. It can be seen that PEG is an easily crystallized polymer. The optical microscope demonstrated that the obtained films gave radiated spherical crystals, namely the chain belts or the crystal chips in spherical crystals assumed a radiated arrangement. With the increased Li⁺ ion concentration, the crystals gradually became small in the order of Fig. 1a–c. It is obvious in Fig. 1d that an irregular black-cross extinction design of a radiated spherical crystal appears in the sight after a single polarized light was added, further proving that a spherical crystallization phenomenon exists in the PEG/Li ionic conduction films.

Figure 2 represents optical and POM photographs of PVDF/PEG composite polymeric ionic conduction films with different mass fractions in the presence of glycerol obtained via a reflected light. Due to compatibility produced through a certain hydrogen bond interaction between the fluorine atom with strong electronegativity in PVDF and an electron acceptor, the hydroxyl hydrogen atom in PEG molecules [13–15], the PVDF/PEG composite film did not present a clear microphase discrete state at a low PVDF content in Fig. 2c. They mutually interlocked. This made microphase domains become thick and the

Fig. 1 Optical (a–c) and POM (d) photographs ($\times 10$) of PEG (molecular weight: 12,000)/Li⁺ polymer films (Li⁺ concentration, mol L⁻¹: a—0.0057; b—0.05; c—0.5; d—0.0057)



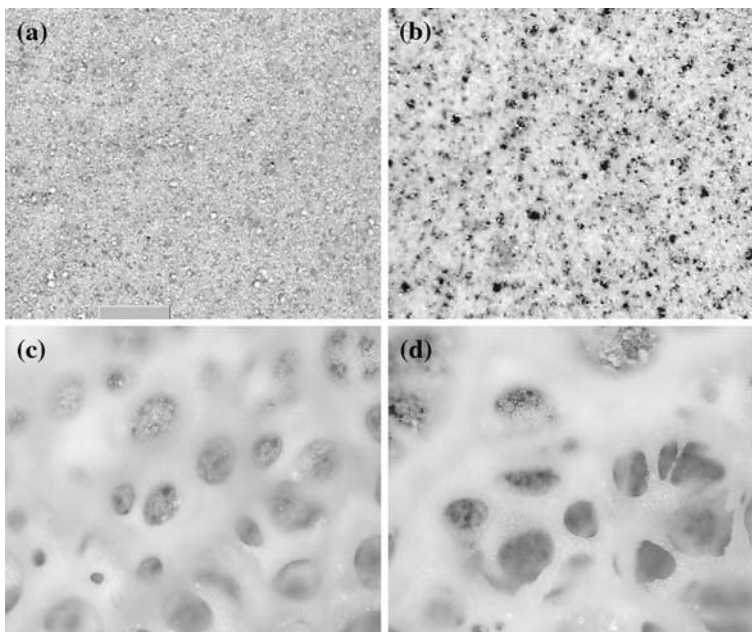
interphases vague, and the extinction phenomenon also even more indistinct (see Fig. 2d). At higher PVDF contents (Fig 2a, b), the phase separation between PEG and PVDF became apparent, and a smaller crystal ball or irregular crystal was formed. The crystal size in micro-phase domains was smaller than that at a low PVDF content (including a single PEG system, cf. Fig. 1) because of the molecular mutual collisions during the growth of PVDF and PEG crystals. On observing the samples in the same visual field with a single polarized light, alternate light and shade patterns were observed in Fig. 2b. But

black-cross extinction phenomena did not appear. By contrast with Fig. 1d, we can further suggest that a small crystal ball or non-spherical crystal polyhedron pattern was formed at a higher content of PVDF owing to the mutual interference between PVDF and PEG molecules.

WAXD analysis

Figure 3 depicts the WAXD patterns of PEG/Li⁺ salt composite polymeric films formed by PEG with different

Fig. 2 Optical (a, c) and POM (b, d) photographs ($\times 20$) of PVDF/PEG with different mass fractions (molecular weight of PVDF/PEG: a and b are 2:1; c and d 0.5:1)



molecular weight. These films have characteristic diffraction designs in the peak positions where 2θ angles are 19.1° , 23.3° , 26.2° , 27° , 28° , and so on, which is in line with the literature [16–18]. With the increased molecular weight, the crystallization diffraction intensity enhanced. This indicated that the PEG molecular chains with molecular weight of 12,000 and 20,000 are easier to arrange regularly, and the chain segments are provided with good flexibility [19] and a higher crystallinity (see Table 1). It is also seen from Fig. 3 that whether the Li^+ salt was added or not did not have an obvious impact on the crystallization diffraction peak positions and peak intensities (curves c and e).

Figure 4 shows the WAXD patterns of PVDF/PEG composite polymeric films with varying constitutional ratios. It was found that a stronger characteristic diffraction peak appeared at 20° , which is ascribed to (110) lattice plane diffraction of clinorhombic PVDF α -crystalline state [23]. The PEG characteristic weak crystallization diffraction peaks appear at the positions of 19.1° , 23.3° , 26.2° for PVDF/PEG films in the absence of glycerol. The diffraction intensities dropped with the PVDF content enhanced. This is because the compatibility between PVDF and PEG that causes the crystallinity to drop. In the meanwhile, for the case of the PVDF/PEG composite polymer electrolyte films with glycerol an additional stronger hydrogen bond mutual affect between PEG and glycerol [12] caused the PEG characteristic diffraction peak to be weaker. Compared with pure PEG films, the half peak width increase implied a smaller crystal grain size. This is consistent with the POM analysis result.

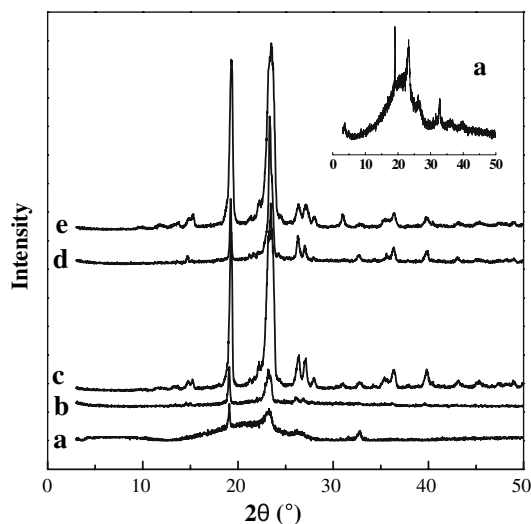


Fig. 3 XRD patterns of PEG/ Li^+ salt composite polymeric films with different molecular weight (a—1,000; b—6,000; c—12,000; d—20,000; e—pure PEG—12,000). The inset shows a XRD pattern of a film in the case of PEG with molecular weight of 1,000

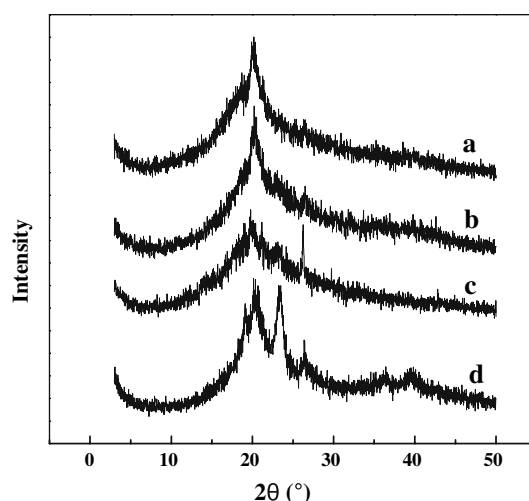


Fig. 4 XRD patterns of PVDF/PEG composite polymeric films (a and b are porous; c and d non-porous. Mass ratio of PVDF/PEG: a and d are 2:1; b and c 0.5:1)

DSC analysis

Figure 5 displays the DSC curves of PEG films with different molecular weight and PVDF/PEG composite polymer films with various mass ratios. Table 1 presents their DSC data. The solid electrolyte film in the presence of PEG showed an unobvious glass transition ranging from -70°C to -30°C and a clear crystalline melting endothermic peak in the range of 38 – 72°C . With increased molecular weight, the glass transition temperature (T_g) and melting temperature (T_m) were enhanced [24]. A similar change was observed in DSC crystallinity except an exceptionally high crystallinity in the case of the PEG with molecular weight of 6,000. This is basically in accordance with the crystallinity results acquired from WAXD measurements (see Table 1). Since the introduction of PVDF would, nevertheless, have impact on PEG crystallization growth, the crystallization degree of the PVDF/PEG composite polymer films was lower than the PEG/ Li^+ polymer film with a corresponding molecular weight (12,000, also see Table 1). The PEG and PVDF crystallization slipped due to the reinforcement of the interaction between PVDF and PEG with the PVDF content enhanced. Especially for the film with a porous surface structure (Fig. 5(B) a, b), the degree of crystallization was even lower than non-porous films. PEG crystallization melting peaks were broadened along with the direction of high temperatures and became unobvious. This further demonstrates that a hydrogen bond between PEG and glycerol has been formed and changed the compatibility each other [12]. Thus the PEG crystallization is undermined, resulting in imperfect crystallization. However, the T_g of PVDF/PEG composite polymer films was deduced owing to the introduction of the

porous structure in the case of glycerol, as shown in Fig. 5(B). It should be noted that the endotherms at about 170 °C are ascribed to the melting of PVDF crystallization. The endothermal intensities in the presence of glycerol (Fig. 5(B) a and b) are lower than those in the absence of glycerol (Fig. 5(B) c and d). They are weakened with the mass ratio of PVDF/PEG increased, similarly owing to the existence of the hydrogen bond at a high PVDF content. These results further support the above description.

ESEM observation

The porous distribution and structure on the surface of PVDF/PEG electrolyte film specimens composed with different mass fractions were observed using ESEM, as displayed in Fig. 6. It is clear that both the phases of PVDF/PEG non-porous films (Fig. 6a, b) and porous films (Fig. 6c–f) exhibited symmetrical distribution. Their interfaces became more obscure, thus giving rise to an incomplete phase separation. The porous structure did not appear on the surface of the films in the absence of glycerol in Fig. 6a, b. However, a little amount of gap existed on the film surface as a result of a relaxed arrangement of two polymer granules. With increased PVDF contents, the granule size and gap became larger. The thickness of the domains was enhanced. The surface configuration,

therefore, became clear. On the other hand, a microporous structure with some density distribution was formed on the surface of the films in the presence of glycerol. With the PVDF content enhancement the phase separation among PVDF, PEG, and glycerol appeared to be obvious. This makes it enriched in the PEG phase because of a stronger hydrogen bond existing between glycerol and PEG molecules [12]. Consequently, the porous–porous connectivity became poor. So although the film surface configuration was improved, the porous number or density significantly reduced. On the contrary, because of the improvement in compatibility resulted from the described-above hydrogen bond, the isolation degree among the pores decreased on the surface of the PVDF/PEG films or the connectivity among each other increased at a higher PEG content. That is to say, a denser porous distribution came up compared with the specimen at a lower PEG content. This elevates the specific area. These phenomena can be clearly observed from the ESEM photographs reduced by 1,000 times in Fig. 6e and f (corresponding to Fig. 6c and d).

Response of PEG/Li⁺ salt solid electrolyte films with various molecular weights

The mentioned-above analyses demonstrate that the PEG/Li⁺ films with different molecular weights present

Fig. 5 DSC curves of (A) PEG (molecular weight of PEG: a—1,000; b—6,000; c—12,000; d—20,000) and (B) PVDF/PEG thin films (Mass ratio of PVDF/PEG: a and c—2:1; b and d—0.5:1. a and b—glycerol, and c and d—no glycerol)

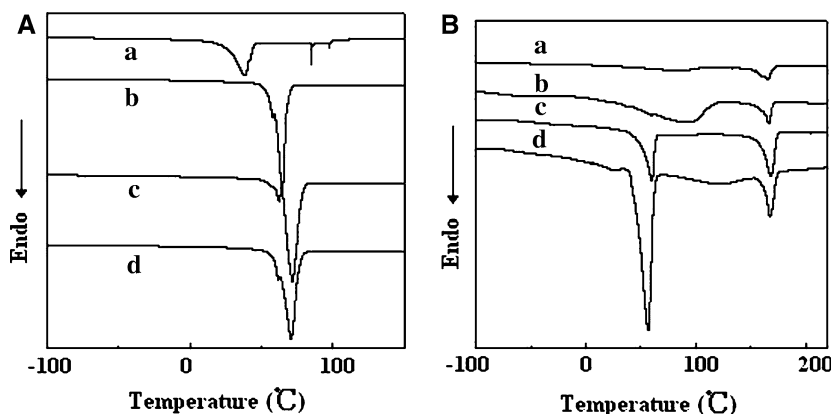


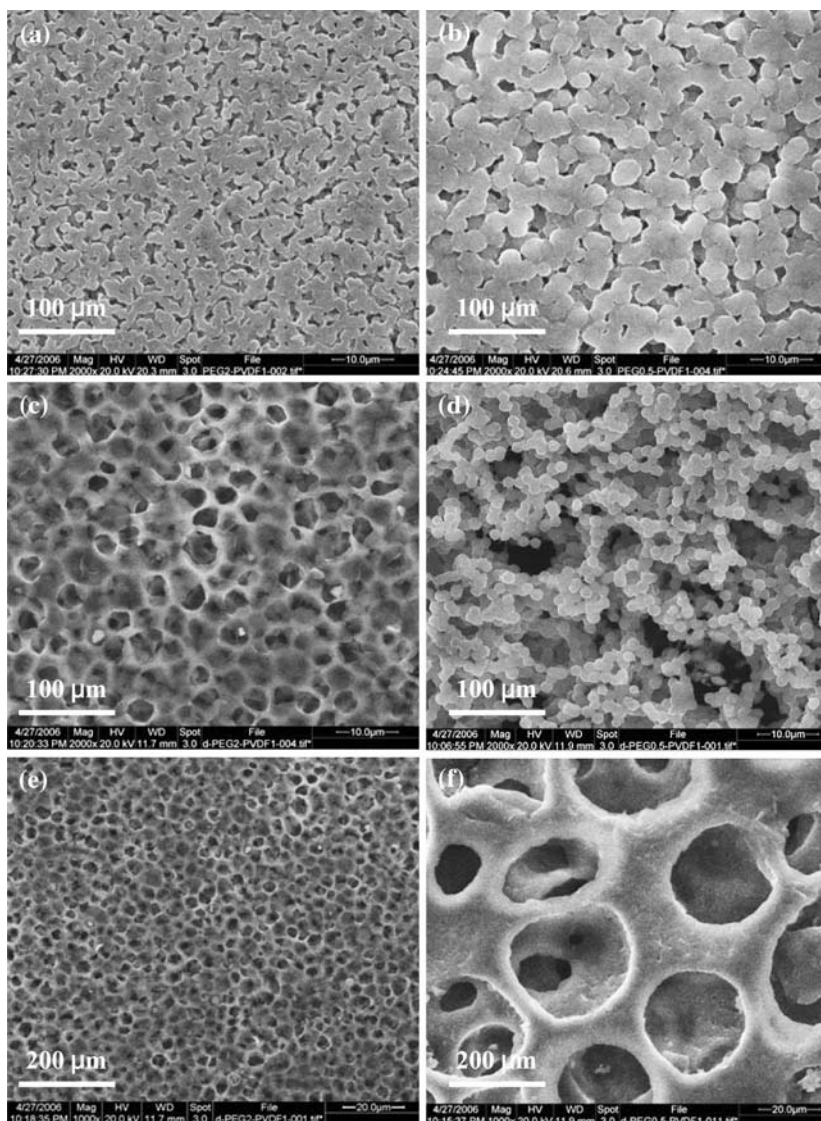
Table 1 DSC data of PEG and PVDF/PEG (12,000) composite polymer films

Molecular weight of PEG	1,000	6,000	12,000	20,000	With pores PVDF:PEG		Without pores PVDF:PEG	
					2:1	0.5:1	2:1	0.5:1
DSC crystallinity ^a , %	62.5	95.2	83.6	85.5	31.52	26.06	52.56	58.31
XRD crystallinity ^b , %	39.26	61.82	74.53	68.12	50.51	42.41	44.85	47.04
T _m , °C	37.97	67.21	70.4	72.09	86/166	84/167	60/169	57/168

^a $X_c = \Delta H_m / \Delta H_m^0 \times 100\%$, where ΔH_m is the fusion enthalpy of crystalline PEG or PVDF in polymer electrolytes, ΔH_m^0 is the heat fusion of 100% crystalline PEG and PVDF, being 213.7 J g⁻¹ and 100 J g⁻¹ [20, 21], respectively

^b Obtained by computer-fitting the XRD spectra in accordance with Gaussian-Cauchy function [22]

Fig. 6 SEM photographs of PVDF/PEG with different mass fractions (Mass ratio of PVDF/PEG: **a, c, and e** are 0.5:1; **b, d, and f** 2:1)



crystalline behavior to some extent. According to the ionic transportation conductive mechanism in amorphous regions, macromolecular materials in the zone will exhibit larger plasticity and form a free volume V_f as a result of the heat movement of molecule chains. When the V_f is large enough, the ions (ClO_4^- and Li^+) will yield certain migration in amorphous zones. Thus the ionic conductance increases. The ionic conductive capacity of polymers can be amended as the following expression (1) [25]:

$$p = \exp(-V/V_f - E_A/kT - W/kT) \quad (1)$$

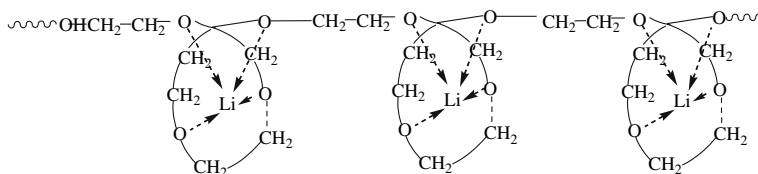
where p is the probability of the free volume exceeding the ionic volume. $-V/V_f$ is related to V_f and T_g . E_A/kT is dependent upon an activated energy as the ion transfers, and W/kT rests with a liberation degree of salt in polymers.

Table 2 shows the influence of the molecular weight of PEG and Li^+ concentrations on resistance of the films. As

shown in Table 2, the resistance at room temperature increased with the molecular weight of PEG enhanced. The value was, however, abnormally high for the PEG-6000 film. This is in accordance with the aforementioned sequence of the increase in crystallinity of the film. The diffusion transportation ionic conductive mechanism through amorphous region deems that the increase in T_g resulted from the increase in molecular weight would cause the V_f to rise, and thus to raise the conductivity at room temperature [26–28]. But the experimental results were in disagreement with the theory. Therefore, we reckon that the conductivity is not only correlated with the movement of a ClO_4^- anion or a Li^+ cation and crystallization behavior of the polymer. This recalled us that the formation of a body centered cubic crystal system similar to AgI crystal may be a key factor yielding high conductive behavior in PEG/ Li^+ crystals, shown in Scheme 1.

Table 2 Influence of molecular weight of PEG and Li^+ concentrations (mol L^{-1}) on resistance of the films

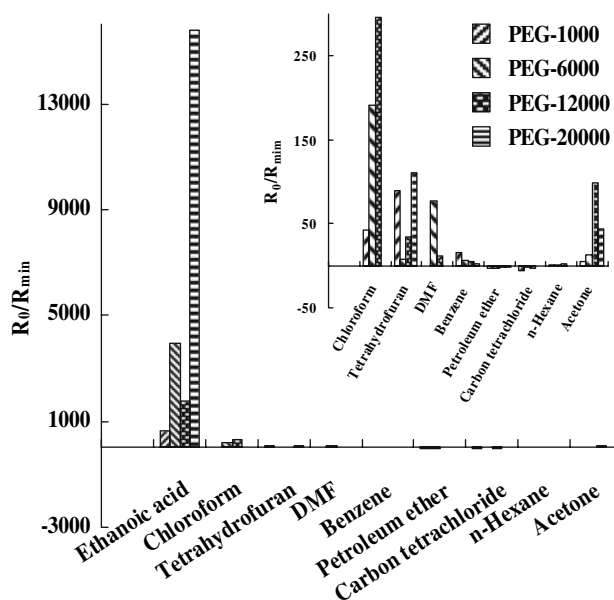
	PEG-1000/ Li^+ 0.0057	PEG-6000/ Li^+ 0.0057	PEG-12000/ Li^+ 0.0057	PEG-20000/ Li^+ 0.0057	PEG-12000/ Li^+ 0.05	PEG-12000/ Li^+ 0.05
R_0 ($\text{M}\Omega$)	40	301	244	346	133	7.56

Scheme 1 Formation model of a polyethylene glycol/ Li^+ salt polymeric composite

Herein, PEG molecular chains form a spiral, Li^+ ions lie in the center of the spiral body. A coordination bond comes into being through a strong coordinating complexation interaction between the oxygen atoms on the hydroxyl groups in PEG and the Li^+ cations in a lithium salt. This coordination complex structure is very conducive to the liberation of ion pairs, forming independent cations and anions and improving the conductivity [25]. Whether the spiral structure exists or not does not affect the formation of the coordination bond. The higher the crystallinity, the stronger the capacity of the coordinating complexation, and the higher the solubility and the solvation ability of lithium perchlorate salts for PEG molecules.

Responsive behavior of the PEG/lithium ion polymeric electrolyte films with different molecular weight was investigated to various solvent vapors, as shown in Fig. 7. It is seen that no matter how the molecular weight of PEG varied, the films all exhibited a high responsive selectivity and sensitivity against polar organic solvents vapor like ethanoic acid, chloroform, THF, DMF, and acetone. This responsiveness appears as a negative vapor coefficient, namely a phenomenon that the resistance of the films declines upon exposed to some vapor environment. The maximal response intensities or responsivities (hereinafter defined as $I = R_0/R_{\min}$, where R_0 is the initial resistance of the film sample and R_{\min} is the minimal resistance after exposed to solvent vapors, which is also referred to as the value of a negative vapor coefficient effect) were followed by 15776.9, 296, 110.5, 77.32, and 99.5 in order of the solvents described above, respectively. The films, however, did not show perceptible responsiveness to non-polarity solvent vapor such as benzene, carbon tetrachloride, petroleum ether, *n*-hexane. Moreover, positive vapor responsiveness was induced upon exposed to petroleum ether and carbon tetrachloride vapor.

It is well known that for composite filled conductive polymeric materials the gas responsiveness can simply be interpreted by an expanding model [29, 30]. They can also

**Fig. 7** Responsivities of several PEG/ Li^+ ion composite polymeric electrolyte films with different molecular weight to various solvent vapors. The inset shows responsivity of the films to any other solvent vapors except for ethanoic acid vapor

be utilized to explain the conductive manner of the compositely ionic conduction polymer films upon exposure to organic solvent vapors [31]. We can group the vapors used for testing conductometric response into three classes: (1) compatible and ionogenic (ethanoic acid), (2) compatible and non-ionogenic (chloroform, THF, DMF, and acetone), and (3) incompatible and non-ionogenic (benzene, carbon tetrachloride, petroleum ether, *n*-hexane). Due to varying swelling extent resulted from different solvent vapors, the free volume V_f for ionic movement will change. As a compatible and ionogenic solvent, the addition of ethanoic acid not only caused plasticization but introduced additional ions (for example, a $-\text{COO}^-$ anion and H^+ cation) that increased the V_f for the ionic diffusion movement and

the number of charge carriers, and improved the conductivity of the polymer electrolyte [32, 33]. On the other hand, as an ionogenic solvent, the oxygen atoms in its $-\text{COO}^-$ group more easily coordinate with Li^+ cations. This promotes the solvation ability for the Li^+ salt and urges the Li^+ ions freely to migrate in the V_f where PEG forms, causing the conductivity drastically to enhance and thus displaying preferred responsiveness.

Indeed, PEG is extremely hydroscopic, but the measuring result shows that an initial resistance in dry air can keep no variation. Therefore, the influence of moisture absorption is negligible. The second group possibly contributed to the plasticization effect only, so the responsivity is low, while the third group had no effect on conductivity. It should be noted that the films display a low positive vapor response characteristic in petroleum ether and carbon tetrachloride (the resistance is slightly enhanced). This is possibly due to some inhibitory action on the formation of the polymer complex compound. These results indicated that the complexing promotion, suppression, and destructive effects from solvents to the PEG/ Li^+ system are important factors affecting the ionic conductivity and responsiveness.

It may also be seen from Fig. 8 that although the response of certain electric conduction films had somewhat deviated, the responsivity of the films with higher molecular weight was still higher on the whole. This is attributed to the higher T_g of the films that causes the V_f of the ions to migrate to increase. Consequently the drop extent of the resistance is high [26–28].

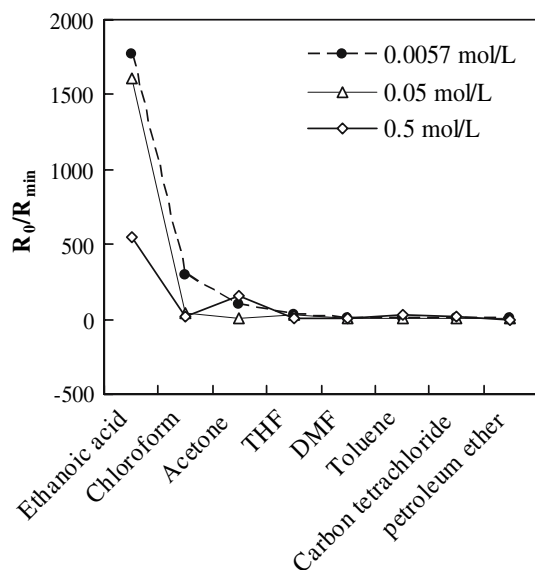


Fig. 8 Dependence of vapor-sensitive behavior of the PEG/ Li^+ salt composite films on Li^+ concentrations

Influence of Li^+ salt concentrations on response

The conductivities of PEG/ Li^+ salt complexing polymer films varied as the Li^+ salt concentrations altered. Figure 8 displays the dependence of vapor-induced conductive behavior of PEG/ Li^+ composite films on Li^+ ion concentrations. It is clear in Fig. 8 that along with the lithium salt concentration increased, the number of charge carrier increased [32], thus gradually increasing the conductivity (also as shown in Table 2) and diminishing the responsiveness to ethanoic acid, chloroform, acetone. However, no obvious variation was observed upon exposed to any other solvent vapor. This is because the crystal grain size changes small (shown as POM observation results in Fig. 1) and the crystallization appears imperfect, causing the free volume at the ionic migration to increase along with the lithium salinity enhancement. On the other hand, the ion migration flux in a unit volume enhances due to a high ClO_4^- and Li^+ density, both causing the improvement in conductivity. It is the high conductivity of PEG/ Li^+ films at the high Li^+ salt concentration that limits the resistance decline space in ethanoic acid vapor and the resistance decline scope became smaller. Correspondingly the responsiveness weakened. Figure 9 shows response patterns of PEG/ Li^+ polymeric electrolyte films with various lithium salt concentrations to ethanoic acid vapor. As presented in Fig. 9, the curves were parallel approximately to x -axis as the electric resistances of the conduction films dropped to 10^5 – $10^6 \Omega$.

Effect of microstructure on conductivity of the films

To explore the influence of the surface microstructure of PVDF/PEG composite electrolytes on the ionic conductive manner, the films with varying mass ratios were prepared

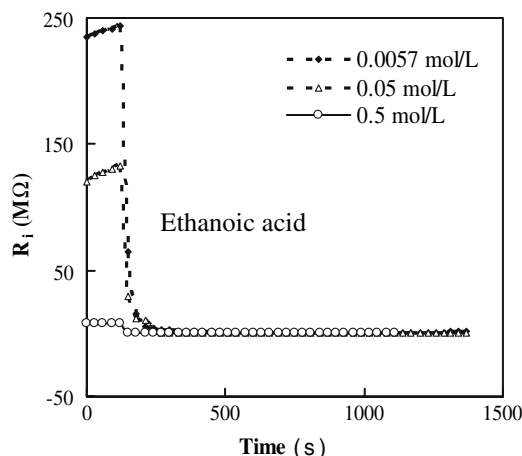


Fig. 9 Response patterns of PEG/ Li^+ polymeric electrolyte films with various Li^+ salt concentrations to ethanoic acid vapor

into micro porous or vesicular surfaces, and resistance response patterns were obtained as shown in Figs. 10 and 11.

It can obviously be seen from Fig. 10 that the resistance rapidly reduces when the compound electrolyte films were exposed to ethanoic acid vapor. The conductivity of the film with micro porous structures dropped with the PVDF content enhanced. This is in agreement with the aforementioned experimental results that the T_g dropped in PEG film measured by DSC. This film produced higher responsiveness toward ethanoic acid vapor at a higher PVDF ratio (see curves a and b in Fig. 10), and also had more obvious responsiveness to THF, chloroform and acetone vapor. In particular the PVDF/PEG microporous film with mass ratio of 2:1 gave the strongest responsiveness to the four kinds of solvents (see Fig. 11). In the case of the ionic conduction films in the absence of glycerol (curves c and d in Fig. 10), the electric conduction behavior was on the contrary to the former along with the PVDF content change because of a higher crystallinity under a low PVDF content (Table 1). But the tendency of the responsivity was consistent. Compared with the electric conduction films with micro pore structure, the conductivity in the absence of glycerol surpassed the former, and its responsivity variation to ethanoic acid vapor is reversible at a low PVDF content. However, the conductivity for the former is slightly lower than the latter while its responsivity is slightly higher than the latter at a high PVDF content.

These performance changes can be explained by the following viewpoints: (1) A micro vesicular structure has a higher specific surface area that can form an electric conduction channel in favor of the lithium ion migration, thus

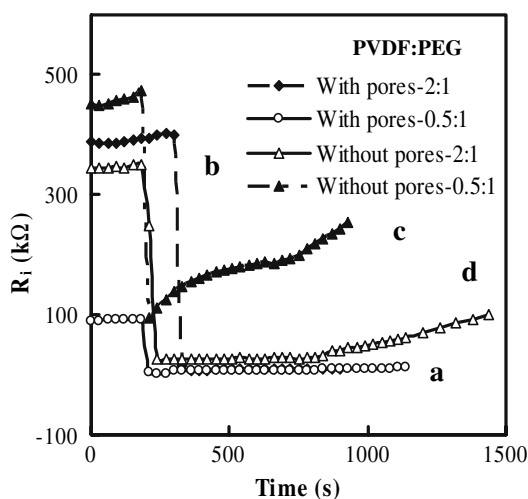


Fig. 10 Effect of surface micro porous structures on response patterns of PVDF/PEG (12,000) Li^+ ion electrolyte films to ethanoic acid (Li^+ concentration: $0.0057 \text{ mol L}^{-1}$)

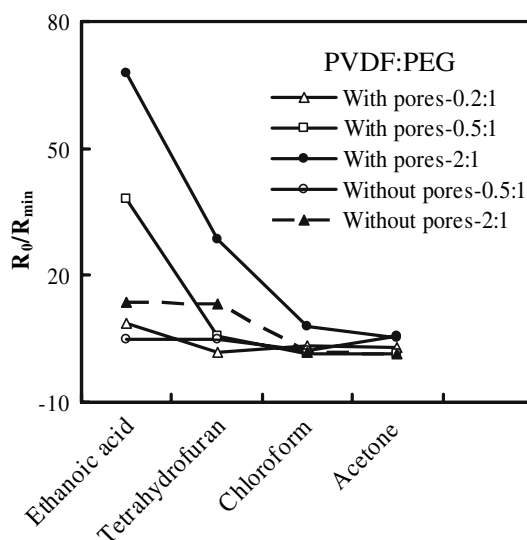


Fig. 11 Effect of the formation of surface micro porous structures on responsivities of PVDF/PEG (12,000) Li^+ ion electrolyte films (Li^+ concentration: $0.0057 \text{ mol L}^{-1}$)

making the conductivity enhance [12, 31]. (2) The poorer pore connectivity, lower pore density and higher crystallinity at a high PVDF content made the amorphous zone and the free volume of the ionic migration reduce, as a result, enhancing the resistance at room temperature. This conclusion is also in accordance with the amorphous region diffusion ionic conduction model. The XRD, SEM results in Figs. 5 and 6 have provided a support for this. A more regular result waits for the further research in the ratio of components.

Conclusions

We have shown that the PEG/ Li^+ composite polymeric film has the advantage of a stronger anti-jamming ability and expected to be exploited as a selective gas sensing material by experimental and theoretical analysis. This conductive material showed high responsive selectivity toward polar organic solvent vapors like ethanoic acid, chloroform, and acetone. In particular, as a compatible and ionogenic matter, ethanoic acid vapors induced large response comparatively to other polar organic solvents. This is mainly ascribed to the following aspects. The addition of ethanoic acid not only caused plasticization but introduced additional ions that increased the V_f for the ionic diffusion movement and the number of charge carriers. Meanwhile, the $-\text{COO}^-$ group can more easily coordinate with Li^+ cations, which promoted the solvation ability and urged the Li^+ ions freely to migrate in the V_f where PEG forms, causing the conductivity drastically to enhance and displaying preferred responsiveness. With the molecular

weight increased the responsivity enhanced. On the contrary, it gave no response or responded weakly to any other non-polar solvent vapors such as benzene, carbon tetrachloride, petroleum ether, and the like. The conductivity and vapor-induced responsive performances or a vapor sensing mechanism of these films are closely related to the crystalline behavior of the materials, T_g , the introduction of an ionogenic analyte and the complexing promotion, restraint and destruction exerted on the PEG/Li⁺ system by solvents. The increase in the Li⁺ salt concentration causes the crystal grain size to wane and the crystals to become imperfect, which in turn expands the V_f for the ionic transference and elevates the ionic migration flux per unit volume, yielding a higher conductivity. Therefore the vapor-induced response of the polymeric films upon exposed to ethanoic acid vapor gradually diminished. The introduction of the micro vesicular structure to a mixed PEG/PVDF composite film may increase its specific surface area, and forms an electric conduction channel propitious to the Li⁺ ionic migration. This makes the value enhance and the responsiveness is distinctly improved. The improvement in pore connectivity and pore density enhancement as well as the drop in crystallinity at a high PEG content makes the amorphous region expand and the free volume of the ionic migration increase, namely the electric conductivity enhancement.

References

- Fenton DE, Parker JM, Wright PV (1973) *Polymer* 14:589
- Meyer WH (1998) *Adv Mater* 10:439
- Tarascon JM, Armand M (2001) *Nature* 414:359
- Amand MB, Chabagno JM, Duclot MJ (1979) *Fast ion transport in solids electrodes and electrolytes*. North-Holland Amsterdam, New York, p 131
- Kim YW, Lee W, Choi BK (2000) *Electrochimica Acta* 45:147
- Zhou H, Gu N, Dong S (1998) *J Electroanal Chem* 441:153
- Dong S, Gu N, Zhou H (1998) *J Electroanal Chem* 441:95
- Qian XM, Gu NY, Cheng ZL (2001) *Electroanal Acta* 46:1829
- Yu WX, Yong SW, Guo GR (1994) *Chin J National Uni Defense Technol* 16:1
- Zhao ZC, Liu K, Zheng H (2005) *Instrument Techn Sens* 3:1
- Xia Y, Lu YL, Sun LC (2005) *Comput Eng Sci* 27:25
- Li J, Xi JY, Song Q, Tang XZ (2005) *Chin Sci Bull* 3:305
- Kumar GG, Kim P, Nahm K, Elizabeth RN (2007) *J Membr Sci* 303:126
- Hilal N, Ogunbiyi OO, Miles NJ, Nigmatullin R (2005) *Sep Sci Technol* 40:1957
- Xu Z, Li L, Wu F, Tan S, Zhang Z (2005) *J Membr Sci* 255:125
- Kim JW, Ji KS, Lee JP, Park JW (2003) *J Power Sources* 119–121:415
- Ahn JH, Wang GX, Liu HK, Dou SX (2003) *J Power Sources* 119–121:422
- Liang XH, Guo YQ, Gu LZ, Ding EY (1995) *Macromolecules* 28:6551
- Chen QC, Deng HY, Ma YM (2002) *Chin Surfactant Detergent Cosmet* 32:2
- Gu NY, Qian XM, Cheng ZL, Jiang JG, Yang XR, Dong SJ (2001) *Chem Res Chin Univ* 22:1403
- Rodgers PA (1993) *J Appl Polym Sci* 50:2075
- Luo YL, Wang GC, Zhang BY, Zhang ZP (1998) *European Polym J* 34:1221
- Liu YX, Luo YL (2006) *Mater Res Innov* 10:52
- Luo J, Wang P, Li J, Xie X, Fan C, He C, Zhong Y (2006) *J Bionic Eng* 23:125
- Zhao WY, Wang YJ (2003) *Functional polymer materials chemistry*, 2nd edn. Chem Ind Press, Beijing, p 53
- Nishio K, Tsuchiya T (2001) *Sol Energ Mat Sol C* 68:295
- Bonino F, Croce F, Panero S (1994) *Solid State Ionics* 70–71:654
- Ikeda Y, Hiraoka T, Ohta S (2004) *Solid State Ionics* 175:261
- Chen J, Tsubokawa N (2000) *Poly Adv Tech* 11:101
- Tsubokawa N, Yukio S, Okazaki M (1999) *Poly Bull* 42:425
- Saito Y, Kataoka H, Stephan AM (2001) *Macromolecules* 34:6955
- Carvalho LM, Guegan P, Cheradame H, Gomes AS (2000) *Eur Polym J* 36:401
- Usami H, Takagi K, Sawaki Y (1992) *J Chem Soc: Faraday Trans* 88:77